



## Development of Active Flow Control for Trucks

Downloaded from: <https://research.chalmers.se>, 2025-06-18 03:33 UTC

Citation for the original published paper (version of record):

Minelli, G., Hartono, E., Chernoray, V. et al (2018). Development of Active Flow Control for Trucks. Proceedings of the Thermal and Fluids Engineering Summer Conference, 2018-March.  
<http://dx.doi.org/10.1615/TFEC2018.tff.021216>

N.B. When citing this work, cite the original published paper.



## **DEVELOPMENT OF ACTIVE FLOW CONTROL FOR TRUCKS**

**G. Minelli,<sup>1,\*</sup> E. Adi Hartono,<sup>1</sup> V. Chernoray,<sup>1</sup> L. Hjelm,<sup>2</sup> B. Basara,<sup>3</sup> S. Krajnović<sup>1</sup>**

<sup>1</sup>Department of Mechanics and Maritime Sciences, Chalmers University of Technology, Gothenburg, Sweden

<sup>2</sup>Volvo Trucks AB, Gothenburg, Sweden

<sup>3</sup>Advanced Simulation Technology, AVL List GmbH, Hans-List-Platz, 8020 Graz, Austria

### **ABSTRACT**

The possibility to actively control the external aerodynamic of vehicles is an attractive yet challenging solution to decrease the aerodynamic drag and the fuel consumption. The work flow that describes the implementation of an Active Flow Control (AFC), for the suppression of the separated flow at the A-pillar of a truck, is summarised in this paper. The presented work spans from a theoretical verification of the method to a preliminary implementation of an AFC on a real full-scale truck cabin. The study involves numerical (CFD) and experimental work, including aerodynamic test in a full scale wind tunnel. The initial CFD simulations of a simplified A-pillar were performed using turbulence resolving numerical method large-eddy simulations (LES). A second step consisted in simulation of a simplified truck cabin using hybrid Partially-Averaged Navier-Stokes simulations (PANS). The AFC was created using synthetic jets produced by the use of loudspeakers mounted in the A-pillars of the model. The numerical and experimental investigations were used to optimise the actuation parameters leading to maximum drag reduction. The final step of the validation of the AFC concept was achieved with a full scale test experimental campaign of a Volvo Truck cabin equipped with the studied AFC device.

**KEY WORDS:** Aerodynamic drag reduction, active flow control, truck aerodynamics, LES, PANS, Partially-Averaged Navier-Stokes, experiment, wind tunnel

### **1. INTRODUCTION**

Road transportation and in particular trucks are needed to improve efficiency, to reduce their power consumption and to contribute to a sustainable mobility. The optimization of the aerodynamic performance have a significant impact on the fuel/power consumption of any road vehicle. In general, road vehicles account for more than 70% of the total transport power consumption, being by far the biggest producer of green house gas. In this scenario, aerodynamic drag plays a major role and it is responsible for the 60% of the total power consumption of a road vehicle. For example, with a medium size car moving at 100 km/h or a semi-truck moving at cruise speed (80 km/h), drag accounts for 80-60% of the total resistance of motion [1–3]. The main objective is therefore to reduce drag, manipulating or better put, controlling the flow to a more desired state, ideally suppressing any separated flow region. This type of practice is called flow control and comprehends different types of tactics. When comes to trucks, extensive aerodynamic research was performed starting from the 1970s [4, 5]. In the early 1980s the front corners of the tractor were smoothed to rounded and flaps bridging the gap between the tractor and the trailer are extensively used today. Flaps applied at the trailing edge [6, 7], flow treatment devices for the under-body [8] or the trailer base [9], cavities and side skirts [10–12],

\*Corresponding G. Minelli: minelli@chalmers.se

boat tails [13] and other add-ons [14] have recently been investigated in order to delay flow separation, thus reducing the wake effect. All these passive flow control techniques have tried to reduce drag with various success, but the challenge of today is to design an active flow control (AFC) that is adjustable to the incoming flow condition. In this study AFC characterized by synthetic jets is investigated. A synthetic jet is a type of jet flow defined by zero net mass flux (ZNMF) and, differently from a pulsating jet [15–18], it is "synthesized" from the surrounding fluid [19]. A synthetic jet flow can be created by plasma actuation [20–23] or by means of the time periodic motion of a flexible diaphragm in a sealed cavity, Fig. 1. Figure 1 shows the working principle of such a device. The periodic sinusoidal motion of the membrane creates a continuous jet flow at the slot defined by a blowing and a suction period. The displacement and the frequency of the diaphragm drive the flow at the slot defining the peak velocity and the period of the sinusoidal jet flow. Due to its versatility and

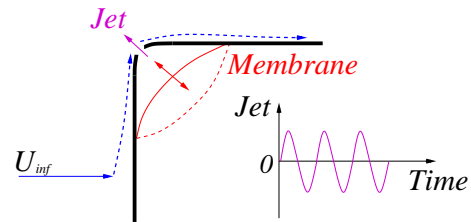


**Fig. 1** A jet flow synthesized by the time periodic motion of a flexible diaphragm in a sealed cavity. The dashed blue lines represent attached flow subjected to flow control.

simplicity the latter technique is developed and integrated in a truck cabin to suppress the separation occurring at the A-pillar, Fig. 2. Normally the flow impinging the front is not oriented along the direction of the truck

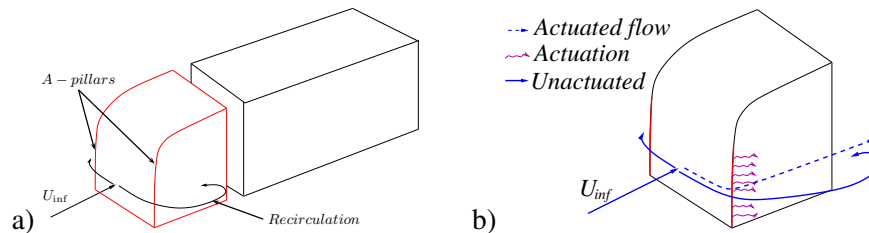


**Fig. 2** The A-pillar (a) and the potential of the actuation (b).

(even when the vehicle is moving at cruise speed), due to side wind, gusts, atmospheric turbulence or steering. In this situation, the truck experiences an angle with respect to the direction of the flow [24–26]. This angle is generally called the yaw angle  $\beta$ . At cruise speed,  $\beta$  varies between  $-10^\circ < \beta < 10^\circ$ , which is sufficient to induce the separation visualized in Fig. 2 even with the use of rounded A-pillar. This paper aims to summarize the work that brought to the implementation of an AFC on a real truck cabin. In particular, the work phases of the process will be shown and the major results of each phase is described. The remainder of the article is organised as follows: chapter 2 briefly explains the methods used during the phases of the work process, the models used and the numerical and experimental set-up. Chapter 3 shows the numerical and experimental results. Conclusions are presented in chapter 4.

## 2. METHODS AND WORK FLOW

The project work flow can be divided into four macro stages. First, large eddy simulations (LES) at low Reynolds number,  $Re = 1 \times 10^5$ , were used to investigate the truck A-pillar separation mechanism and its control. The computational domain consisted of a longitudinal section of a simplified truck model, Fig. 3. The flow was sampled over time (blue rectangle in Fig. 3b) and proper orthogonal decomposition (POD) [27] and fast Fourier transform analysis were used to post process the data sampled. For further numerical details of the LES refer to [28].

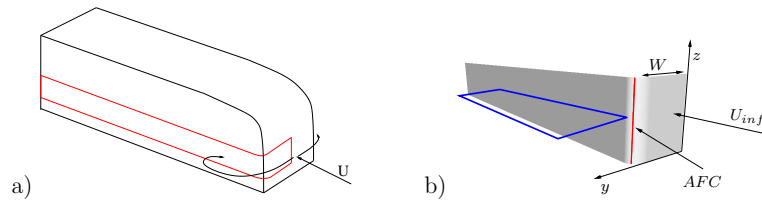


**Fig. 3** a) The longitudinal section of a simplified truck. b) The computational model. The blue rectangular area indicates the observed domain.

Second, a simplified truck cabin, Figs. 4 and 5, is designed to contain four loud speakers that work as a flexible diaphragm in a sealed cavity (refer to Fig. 1). Figure 4 shows the assembly process of the model, while Fig. 5 shows the working principle of the actuation. The experimental work was conducted at the Chalmers University closed loop wind tunnel (WT) at moderate  $Re = 5 \times 10^5$ . Time resolved particle image velocimetry (PIV) and pressure measurements were used to observe the unactuated and actuated flow around the model. For further details of the experimental methods used refer to [29]

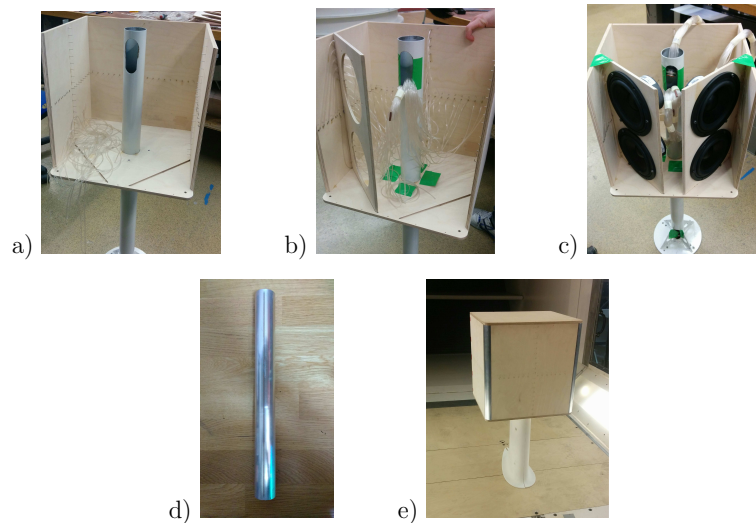


**Fig. 4** a) The side and the rear faces of the cabin are assembled. b) The pressure taps piping and the loud speaker's support. c) The loud speakers in place. d) The aluminium cylinder representing the A-pillar of the truck cabin. The cylinder has a 1mm slit to allow the actuation. e) The model is placed in the WT.

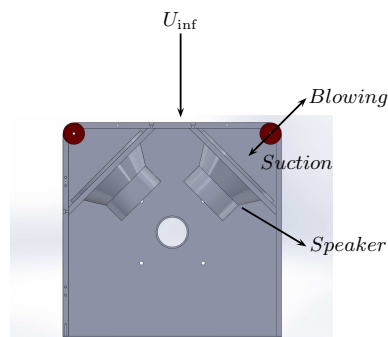


**Fig. 5** The working principle of the loud speaker flexible diaphragms.

Third, the partially averaged Navier-Stokes (PANS) [30] numerical method has been validated against resolved LES and previous experiments (phase 2). The details of the validation are reported in [31]. After the validation, PANS was used to simulate realistic flow conditions characterized by gusts at moderate  $Re = 5 \times 10^5$ . To reproduce this phenomenon, the model is forced to oscillate with a yaw angle  $10^\circ > \beta > -10^\circ$  and a non-dimensional frequency  $St = fW/U_{inf} = 0.1$ , Fig. 6a. The numerical domain used for these simulations and its main dimensions are presented in Fig. 6b and Tab 1. PANS were employed for the numerical study

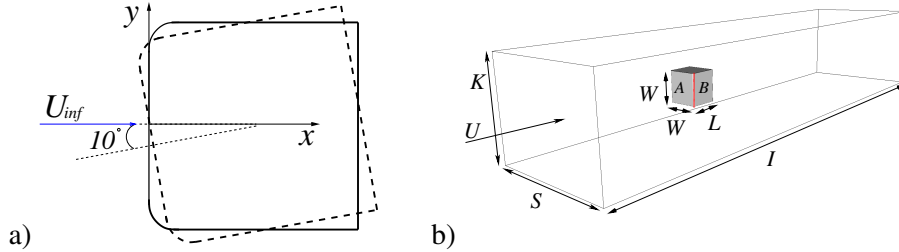


**Fig. 6** a) Top view of the rotation of the model during the simulation. b) The numerical domain.

**Table 1** Dimension of the computational domain. All dimensions are scaled by the model width  $W = 0.4\text{m}$ .

$G$	$L$	$I$	$K$	$S$	$R$
0.0025	0.9	17.5	3	4.5	0.05

of the AFC, while LES was used for a more complete validation of the first method. The following boundary conditions were applied to all simulations. A homogeneous Neumann boundary condition was applied at the outlet. The surfaces of the body and the wind tunnel walls were treated as no-slip walls. A time varying velocity, Eq. 1, reproduced the jet flow described by Fig. 1.

$$U_{afc} = 0.26U_{inf} \sin(t2\pi f_a), \quad (1)$$

When the flow is unactuated, the AFC surface was defined as a no-slip wall, likewise the rest of the body. The deformation of the grid was made only in a circular region around the model (within a non dimensional radius  $R_{def}/W = 2.5$ ).

The last phase consists in the implementation of the AFC so far described in a real truck cabin at realistic  $Re = 3.5 \times 10^6$ . A test case truck cabin was thus provided by Volvo Trucks to test the actuation methodology. The flow control methodology was implemented in a modified version of a truck cabin, Fig. 7 (left) and later tested in the Canada National Research Council full scale facility. The flow is analysed by means of tufts visualization superimposed on the lateral window, Fig. 7 (right).



**Fig. 7** Left, the Volvo Truck cabin positioned in the test section. Right, a zoom in of the slot created at the A-pillar. The loudspeaker are embedded in a sealed cavity in the interior of the cabin.

### 3. RESULTS

Following the same pattern described in the previous chapter (division of the work in four phases), the results achieved in each phase are briefly described here. The purpose of this chapter is then to collect the most important results that characterize the process to develop an AFC for heavy vehicles, from a preliminary numerical study to its implementation in a real truck cabin.

Phase 1 significantly contributes to a better understanding of the separation mechanism of the flow and of the frequencies that play a major role in the dynamic of the structures. Phase 1 also defines the guidelines for the AFC to be effective. In particular, it was found that two main frequencies play a major role in the unactuated flow: the near wake structures (black eddies represented in Fig. 8) frequency and the shear layer structures (red eddies in Fig. 8) frequency. Tuning the actuation of the AFC to the shear layer frequency, the highest reduction of the recirculation bubble was achieved, Fig. 9. For the validation of the numerical simulations and further numerical details of the LES refer to [28].

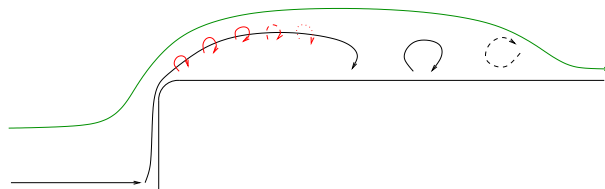


**Fig. 8** The flow topology of the separation mechanism. In red the shear layer structures. In black the larger near wake structures and in green a streamline of the averaged field indicating the dimension of the recirculation bubble.

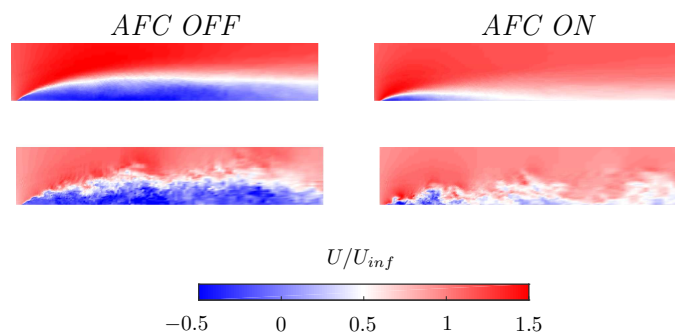


**Fig. 9** LES simulation results, averaged and instantaneous stream-wise velocity. Left, unactuated flow. Right, actuated flow using the shear layer frequency.

Phase 2 demonstrates the reproducibility of the actuation in WT experiments, Fig. 10. Also in this case the most effective frequency that suppresses the separation bubble is the shear layer structures frequency. For a better understanding of the wind tunnel set-up and further experimental details refer to [29].

In phase 3 the accuracy of PANS was first proved for the model used in the WT experiments of phase 2 and secondly used to simulate the effectiveness of AFC under severe flow condition. Figure 11 shows the effectiveness of the AFC under periodic gusts. The  $C_d$  value is reduced throughout the entire yaw angle  $\beta$  sweep and the hysteresis of the lateral force coefficient  $C_s$  is reduced, indicating an improved lateral stability. For the validation of the numerical simulations and further numerical details of the PANS method refer to [31].

After the previous three preliminary phases, the last phase aims to implement the AFC in a real truck cabin. All previous results have shown the effectiveness of such a flow control and this results is confirmed by tuft visualization on the side window of the full case cabin, Fig. 12. In fact, a full scale experimental campaign was conducted and Fig. 13 shows the averaged flow streamlines on the surface of the model and highlights the

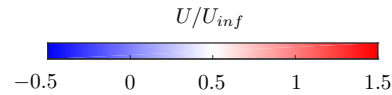


**Fig. 10** Time resolved PIV results. Left, unactuated flow. Right, actuated flow using the shear layer frequency. Right side, streamlines of the averaged flow field. Left side, a snapshot of the instantaneous stream-wise velocity field.

**Fig. 11** Top, isosurface of the second invariant of the velocity coloured by the stream-wise flow velocity. Unactuated (left) and actuated (right) cases.  $\beta = 5^\circ$  clock wise rotation. Bottom,  $C_d$  (left) and  $C_s$  (right). Comparison between the static (dots) and the dynamic unactuated (solid line) case.

reduction of the recirculation bubble when the AFC is actuated. Tufts were positioned on a black surface to improve the quality of the picture and facilitate the post processing of the data. Figure 12 shows a consecutive zoom of the area of interest that was investigated. Each tuft is attached with a red sticker, which is 15mm in diameter and approximately 0.3mm in thickness. The length of the tufts is about 35mm. The tuft diameter used is approximately 1mm. Figure 13 shows post processed images of the observed area of two different cases: the pictures in the left column show the unactuated flow, while the pictures in the right column show the actuated flow case. A script was developed to post process the instantaneous pictures that captured tufts oscillations. Every set of pictures (500 snapshots) was first averaged for a traditional tufts analysis, Fig. 13(a-b). Higher perturbation regions show larger fluctuation of the interested tufts, resulting in a larger effective average tuft cone visualization. The averaged images are further post processed for a clearer flow visualization. The vector field represented by the direction of each tuft is superimposed in Fig. 13(c-d) and flow streak-lines

are presented in Fig. 13(e-f). The analysis shows the benefit of the installed AFC. When the AFC is actuated, the flow is redirected along the stream-wise direction, and no reverse flow is visualised on the side of the truck. On the other hand, when the AFC is off, the flow is characterized by a strong vertical component and reverse flow.

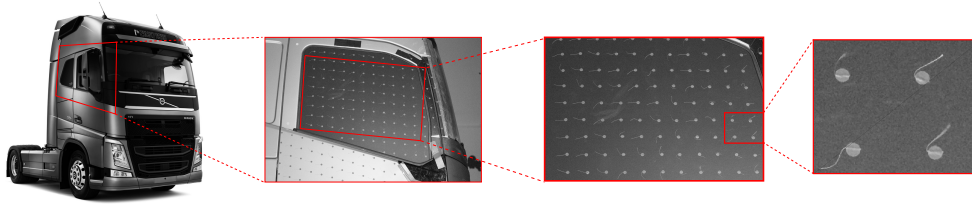


**Fig. 12** A zoom of the observed domain. The tufts position is averaged and analysed over time.

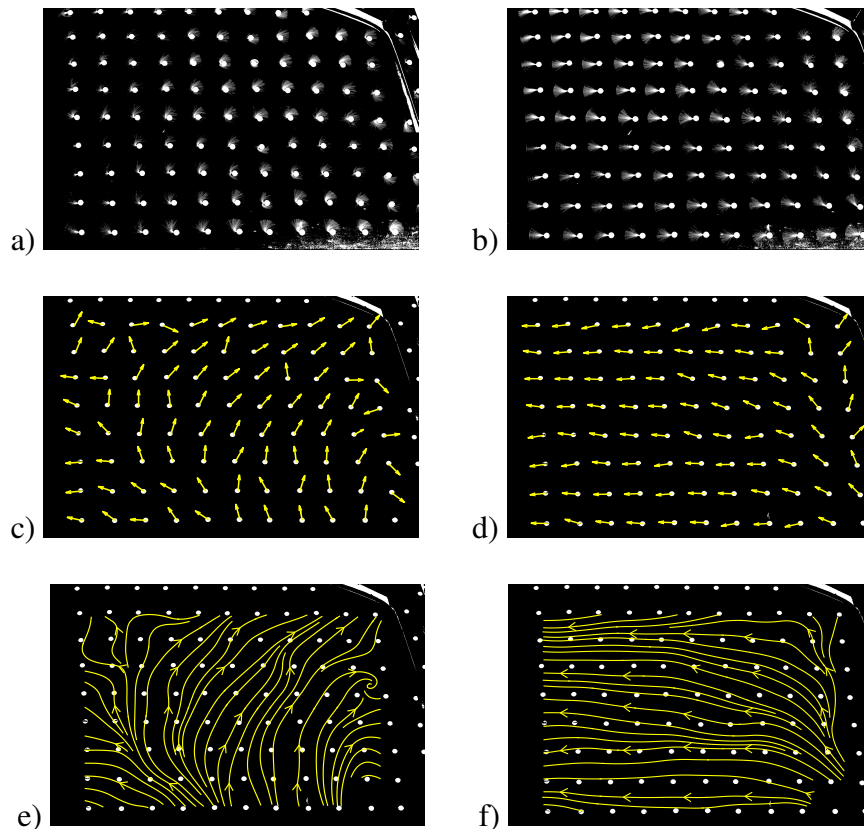


**Fig. 13** Average tufts tracking (a-b). Vector field visualization (c-d) and streak-lines (e-f); reconstruction from the average tuft tracking. AFC off (a, c and e). AFC on (b, d and f).

#### 4. CONCLUSIONS

Here it has been described the importance and the potential of an AFC when applied to road vehicles. The development of this technique and its effectiveness were tackled using both numerical simulation and wind tunnel experiments. The AFC achievements observed in numerical simulations were corroborated by experimental data, and the conceptual flow structure mechanism found its counterpart in the analysis of the aerodynamic performance of a real vehicle.

First, LES demonstrated the efficacy of the AFC in a very simplified case. Even though the model used for the simulations was removed from geometrical complexities, the study gave important directions for the design of

the experimental demonstrator model (representative of a truck cabin) equipped with AFC. The AFC ability to improve the aerodynamic performance of the model was remarkable. Moreover, the interaction between the actuation and the surrounding flow is crucial for a successful implementation. The AFC actuation frequency and magnitude are in fact the main players in the game and they need to be tuned toward an optimal flow control.

Second, a consistent study of PANS was conducted. PANS is a promising numerical tool that blends the accuracy of an LES with the efficiency of RANS. As such, the method was tested and validated against LES and WT experiments. The results show good agreement with experimental data. Therefore, PANS was used to simulate a controlled flow under the effect of gusts. The AFC was demonstrated to improve the aerodynamic performance under discussed flow conditions as well.

Third, the flow control was implemented and tested on a real Volvo truck cabin. At this stage, the same AFC principle used for the demonstrator was applied here. Tufts flow visualizations confirm the beneficial effect of the AFC.

In conclusion, the stages covered so far show promising AFC results in terms of drag reduction and also show the possibility for an extensive applicability of AFC for road vehicles. Nevertheless, smaller and more efficient devices need to be investigated for a real implementation. An investigation of micro-blowers is ongoing and, once their robustness is tested, they would be a good candidate for a broader implementation.

## ACKNOWLEDGMENTS

This work is funded by the Swedish Energy Agency and supported by Volvo Trucks. Software licenses were provided by AVL List GMBH. Computations were performed at SNIC (the Swedish National Infrastructure for Computing) at the National Supercomputer Center (NSC) at LiU.

## REFERENCES

- [1] A. Roshko, "Perspectives on bluff body aerodynamics," *Journal of Wind Engineering and Industrial Aerodynamics*, vol. 49, no. 1, pp. 79–100, 1993.
- [2] H. Choi, J. Lee, and H. Park, "Aerodynamics of Heavy Vehicles," *Annual Review of Fluid Mechanics*, vol. 46, pp. 441–468, 2014.
- [3] T. C. Schuetz, *Aerodynamics of Road Vehicles, Fifth Edition*. SAE International, dec 2015.
- [4] K. Cooper, "The effect of front-edge rounding and rear-edge shaping on the aerodynamic drag of bluff vehicles in ground proximity," 1985.
- [5] K. Cooper, "Truck Aerodynamics Reborn - Lessons from the Past," *SAE Technical Paper Series*, 2003.
- [6] M. El-alti, V. Chernoray, M. Jahanmiri, and L. Davidson, "Experimental and Computational Studies of Active Flow Control on a Model Truck-trailer," *EPJ Web of Conferences 25*, vol. 010, 2012.
- [7] J. Kehs, K. Visser, J. Grossmann, C. Horrell, and A. Smith, "Experimental and Full Scale Investigation of Base Cavity Drag Reduction Devices for Use on Ground Transport Vehicles BT - The Aerodynamics of Heavy Vehicles III: Trucks, Buses and Trains," pp. 269–283, Cham: Springer International Publishing, 2016.
- [8] R. Pankajakshan, C. B. Hilbert, and D. L. Whitfield, "Passive Devices for Reducing Base Pressure Drag in Class 8 Trucks BT - The Aerodynamics of Heavy Vehicles III: Trucks, Buses and Trains," pp. 227–235, Cham: Springer International Publishing, 2016.
- [9] R. Wood and S. Bauer, "Simple and low-cost aerodynamic drag reduction devices for tractor-trailer trucks," *SAE transactions*, vol. 112, no. 2, pp. 143–160, 2003.
- [10] B. Khalighi, S. Zhang, C. Koromilas, S. R. Balkanyi, L. P. Bernal, G. Iaccarino, and P. Moin, "Experimental and Computational Study of Unsteady Wake Flow Behind a Bluff Body with a Drag Reduction Device," *Society of automotive engineers*, no. 724, pp. 1–15, 2001.
- [11] R. Verzicco, M. Fatica, G. Iaccarino, P. Moin, and B. Khalighi, "Large Eddy Simulation of a Road Vehicle with Drag-Reduction Devices," *AIAA Journal*, vol. 40, no. 12, pp. 2447–2455, 2002.

- [12] G. M. R. van Raemdonck and M. J. L. van Tooren, "Numerical and Wind Tunnel Analysis Together with Road Test of Aerodynamic Add-Ons for Trailers BT - The Aerodynamics of Heavy Vehicles III: Trucks, Buses and Trains," pp. 237–252, Cham: Springer International Publishing, 2016.
- [13] J. D. Coon and K. D. Visser, "Drag Reduction of a Tractor-Trailer Using Planar," *The Aerodynamic of Heavy Vehicles: Trucks, Buses, and Trains*, vol. 1, 2004.
- [14] S. Krajnović, "Large Eddy Simulation Exploration of Passive Flow Control Around an Ahmed Body," *ASME Journal of Fluids Engineering*, vol. 136, p. 121103, sep 2014.
- [15] S. Krajnović, J. Östh, and B. Basara, "LES study of breakdown control of A-pillar vortex," *International Journal of Flow Control*, vol. 2, pp. 237–258, 2010.
- [16] D. Barros, J. Borée, B. R. Noack, A. Spohn, and T. Ruiz, "Bluff body drag manipulation using pulsed jets and Coanda effect," *Journal of Fluid Mechanics*, vol. 805, pp. 422–459, 2016.
- [17] G. Lubinsky and A. Seifert, "Suction and Oscillatory Blowing Applied to the Rounded Front Edges of a Square Prism BT - Instability and Control of Massively Separated Flows: Proceedings of the International Conference on Instability and Control of Massively Separated Flows, held in P," pp. 157–162, Cham: Springer International Publishing, 2015.
- [18] A. Seifert, I. Dayan, C. Horrell, J. Grossmann, and A. Smith, "Heavy Trucks Fuel Savings Using the SaOB Actuator BT - The Aerodynamics of Heavy Vehicles III: Trucks, Buses and Trains," pp. 377–390, Cham: Springer International Publishing, 2016.
- [19] B. L. Smith and A. Glezer, "The formation and evolution of synthetic jets," *Physics of Fluids (1994-present)*, vol. 10, no. 9, pp. 2281–2297, 1998.
- [20] E. Moreau, "Airflow control by non-thermal plasma actuators," *Journal of Physics D: Applied Physics*, vol. 40, no. 3, pp. 605–636, 2007.
- [21] T. C. Corke, C. L. Enloe, and S. P. Wilkinson, "Dielectric Barrier Discharge Plasma Actuators for Flow Control," *Annual Review of Fluid Mechanics*, vol. 42, no. 1, pp. 505–529, 2010.
- [22] N. Benard and E. Moreau, "Electrical and mechanical characteristics of surface AC dielectric barrier discharge plasma actuators applied to airflow control," *Experiments in Fluids*, vol. 55, no. 11, 2014.
- [23] J. A. Vernet, *Plasma actuators for separation control on bluff bodies*. PhD thesis, Mechanics, School of Engineering Sciences (SCI), KTH, 2017.
- [24] S. Watkins and J. W. Saunders, "Turbulence Experienced by Road Vehicles under Normal Driving Conditions," *SAE Technical Paper Series*, 1995.
- [25] S. Wordley and J. Saunders, "On-road Turbulence," 2008.
- [26] S. Wordley and J. Saunders, "On-road Turbulence: Part 2," vol. 2, no. 1, pp. 111–137, 2009.
- [27] L. Sirovich, "Turbulence and the dynamics of coherent structures part i: coherent structures," *Quarterly of Applied Mathematics*, vol. XLV, no. 3, pp. 561–571, 1987.
- [28] G. Minelli, S. Krajnović, B. Basara, and B. R. Noack, "Numerical Investigation of Active Flow Control Around a Generic Truck A-Pillar," *Flow, Turbulence and Combustion*, vol. 97, no. 4, pp. 1235–1254, 2016.
- [29] G. Minelli, E. A. Hartono, V. Chernoray, L. Hjelm, and S. Krajnović, "Aerodynamic flow control for a generic truck cabin using synthetic jets," *Journal of Wind Engineering and Industrial Aerodynamics*, vol. 168, pp. 81–90, 2017.
- [30] B. Basara, S. Krajnović, and S. Girimaji, "PANS methodology applied to elliptic-relaxation based eddy viscosity transport model," *Turbulence and Interactions*, pp. 63–69, 2010.
- [31] G. Minelli, E. Adi Hartono, V. Chernoray, L. Hjelm, S. Krajnović, and B. Basara, "Validation of PANS and active flow control for a generic truck cabin," *Journal of Wind Engineering and Industrial Aerodynamics*, vol. 171, pp. 148–160, 2017.